Supplementary Material for

Electrorheology of a dilute emulsion of surfactant-covered drops

Antarip Poddar[1], Shubhadeep Mandal[1,2], Aditya Bandopadhyay*[1], and Suman Chakraborty†[1]

[1]Department of Mechanical Engineering, Indian Institute of Technology Kharagpur, Kharagpur, West Bengal - 721302, India

[2]Max Planck Institute for Dynamics and Self-Organization, Am Fassberg 17, D-37077 Göttingen, Germany

May 22, 2019

S-1. Growing and decaying spherical harmonics

The different growing and decaying harmonics appearing in the general expression of the hydrodynamic field variables can be expressed as

$$\left.\begin{aligned} p_n &= \lambda r^n \sum_{m=0}^{n} \left[A_{n,m}\cos(m\phi) + \hat{A}_{n,m}\sin(m\phi)\right] P_{n,m}(\eta) \\ \Phi_n &= r^n \sum_{m=0}^{n} \left[B_{n,m}\cos(m\phi) + \hat{B}_{n,m}\sin(m\phi)\right] P_{n,m}(\eta) \\ \chi_n &= r^n \sum_{m=0}^{n} \left[C_{n,m}\cos(m\phi) + \hat{C}_{n,m}\sin(m\phi)\right] P_{n,m}(\eta) \end{aligned}\right\} \tag{S-1}$$

$$\left.\begin{aligned} p_{-n-1} &= r^{-n-1} \sum_{m=0}^{n} \left[A_{-n-1,m}\cos(m\phi) + \hat{A}_{-n-1,m}\sin(m\phi)\right] P_{n,m}(\eta) \\ \Phi_{-n-1} &= r^{-n-1} \sum_{m=0}^{n} \left[B_{-n-1,m}\cos(m\phi) + \hat{B}_{-n-1,m}\sin(m\phi)\right] P_{n,m}(\eta) \\ \chi_{-n-1} &= r^{-n-1} \sum_{m=0}^{n} \left[C_{-n-1,m}\cos(m\phi) + \hat{C}_{-n-1,m}\sin(m\phi)\right] P_{n,m}(\eta) \end{aligned}\right\}, \tag{S-2}$$

where $P_{n,m}(\eta)$ stands for the associated Legendre polynomial of degree n and order m with an argument, $\eta = \cos(\theta);\ A_n, B_n, C_n, A_{-n-1}, B_{-n-1}, C_{-n-1},\ \hat{A}_n, \hat{B}_n, \hat{C}_n, \hat{A}_{-n-1}, \hat{B}_{-n-1}$ and $\hat{C}_{-n-1}$

*Email: aditya@mech.iitkgp.ernet.in

†Email: suman@mech.iitkgp.ernet.in

are the arbitrary constant to be determined by solving the surfactant transport equation and the hydrodynamic boundary conditions at the drop-matrix interface.

S-2. Comparison with previous works

In different steps of calculation, the expressions of important physical variables have been validated against various limiting cases of the present physical situation, as elaborated below:

(i) *Surfactant-free drop in shear flow:*

This simplistic case can be obtained in the present study by substituting $M = 0$ and $\beta = 0$ in the resulting expressions. Under such a condition the leading order effective shear viscosity was first obtained by Taylor (1932). Our leading order results in equation (14) of the main manuscript, i.e. $\eta^{(0)}_{\text{h,clean}} = 1 + \nu\dfrac{(5\,\lambda + 2)}{(2\,\lambda + 2)}$, corroborates with that classic result.

In the same limit, we obtained the $O(Ca)$ normal stress differences as given below:

$$N_1^{(Ca)} = \nu\frac{(16 + 19\,\lambda)^2}{40\,(\lambda + 1)^2} \tag{S-3a}$$

and

$$N_2^{(Ca)} = -\nu\frac{551\,\lambda^3 + 1623\,\lambda^2 + 1926\,\lambda + 800}{280\,(\lambda + 1)^3}. \tag{S-3b}$$

Also in $O(Ca)$, the hydrodynamic contribution to the effective shear viscosity is obtained as zero ($\eta_{\text{eff}}^{(Ca)} = 0$). These observations are in agreement with the seminal work of Schowalter *et al.* (1968). For similar conditions, the $O(Ca)$ shape function $f^{(Ca)}$ matches with the expressions obtained by Barths-Biesel & Acrivos (1973) and Vlahovska (2011), respectively.

(ii) *Surfactant-coated drop in shear flow:*

The expressions in the vanishing diffusion regime or the high surface Péclet number regime ($Pe_S \gg 1$) (Vlahovska *et al.*, 2009) can be obtained by taking a limit $k \to \infty$ and substituting $M = 0$ in the present expressions, as shown below:

$$N_1^{(Ca)} = \frac{5\,\nu\,(3\beta + 1)}{2\beta} \tag{S-4a}$$

and

$$N_2^{(Ca)} = -\frac{5\,\nu\,(6\,\beta + 7)}{28\,\beta}. \tag{S-4b}$$

In the diffusion dominated limit (i.e. $Pe_S \ll 1$) if we substitute $M = 0$ in the presently obtained surfactant concentration $\Gamma = \Gamma^{(0)} + Ca\,\Gamma^{(Ca)}$ and $O(Ca)$ drop shape correction $f^{(Ca)}$, they become similar to those obtained by Mandal *et al.* (2017). In all these our calculations consistently capture the result of $N_2 < 0$ in the absence of electrical effects. This is commonly observed in polymeric solutions and has been reported by earlier studies Li & Pozrikidis (1997).

(iii) *Uncontaminated drop in combined shear flow and electric field:*

In the limit $\beta \to 0$ the surface tension becomes uniform along the drop surface. For that situation, the present results e.g. the drop deformation, effective shear viscosity and normal stress differences in various orders of perturbation, match exactly with those of Mandal & Chakraborty (2017). When the electric field is applied along the direction of velocity gradient $\Phi_t = \pi/2$, we find that in equation (14) of main manuscript, the clean drop effective viscosity due to electric field ($\eta^{(0)}_{\mathrm{e,clean}}$) vanishes. A similar observation was also made in another reported work (Vlahovska, 2011). The electric field contribution, to the normal stress differences in the leading order (equation (15) of the main manuscript), are also in agreement with them.

Hence we obtained a reasonable confidence on the correctness of the theoretical analysis presented in this work.

S-3. Effect of β and k on surface concentration and surface tension

Here in figure S-1, we explore the role of the surfactant characterization parameters, namely the elasticity number β and physicochemical constant k, in altering the surfactant concentration and surface tension variation on the drop surface.

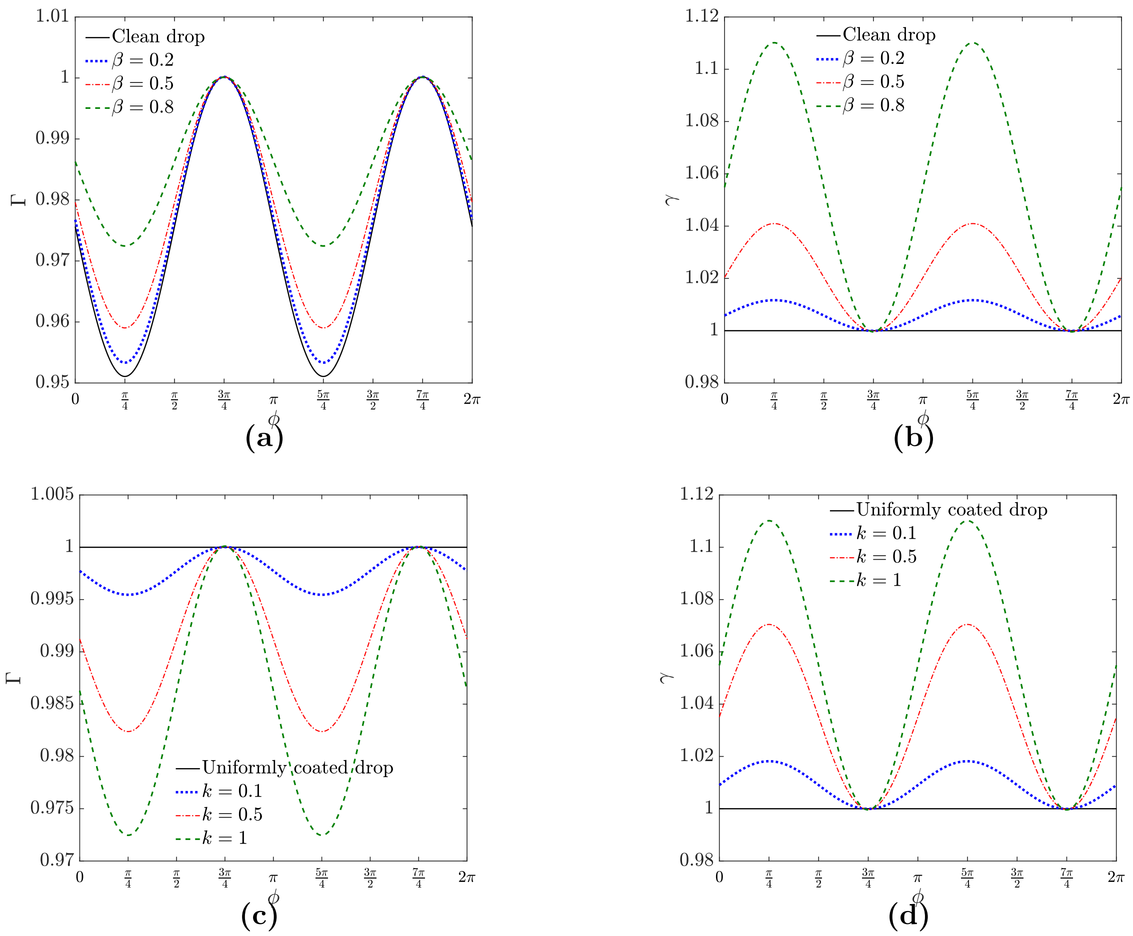

Figure S-1: Variation of surfactant concentration $\left(\Gamma = \Gamma^{(0)} + Ca\,\Gamma^{(Ca)}\right)$ and interfacial tension $\left(\gamma = \gamma^{(0)} + Ca\,\gamma^{(Ca)}\right)$ in the $x-y$ plane for different values of the parameters β and k. In sub-figures (a) and (b), $k = 1$ is chosen while $\beta = 0.8$ is taken for (c) and (d). Here the tilt angle of the electric field is $\Phi_t = \pi/4$, Mason number $M = 2$ and other parameters are as per system-C.

S-4. Effect of Mason number on surface tension

In figure S-2 we delineate the effects of strength of electrical stresses relative to the hydrodynamic stresses, by varying the Mason number, define as $M = \dfrac{\epsilon_c \widetilde{E}_\infty^2}{\mu_c \widetilde{G}}$.

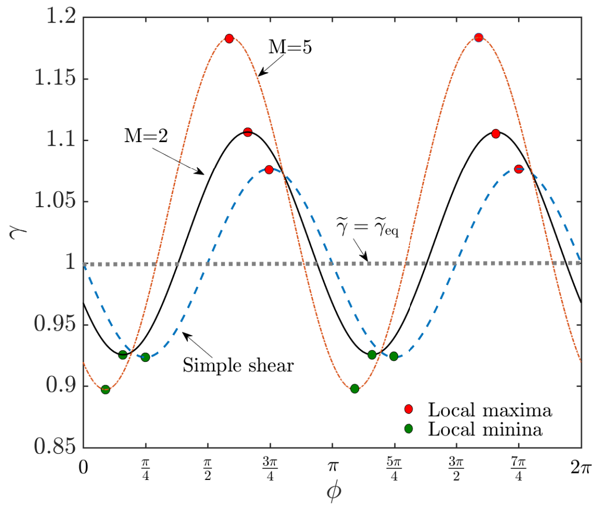

Figure S-2: Interfacial tension variation (γ) in the $x - y$ plane for different Mason number (M). Here $\beta = 0.8, k = 1$ and $\Phi_t = \pi/2$. Other parameters are chosen following system-A.

S-5. Interplay between charge convection and surfactant transport

In figure S-3(a), we demonstrate the variations in the surface charge distribution ($q_S = q_S^{(0)} + Re_E\, q_S^{(Re_E)}$) for different values of the surface elasticity parameter β. It is observed that for a surfactant-contaminated drop, the redistribution of charges due to the presence of finite charge convection at the interface is affected by the Marangoni effects. On the other hand, the modulations in the electrohydrodynamic flow, created by the finite charge convection, interplay with the Marangoni convection. This behavior is depicted in figure S-3(b).

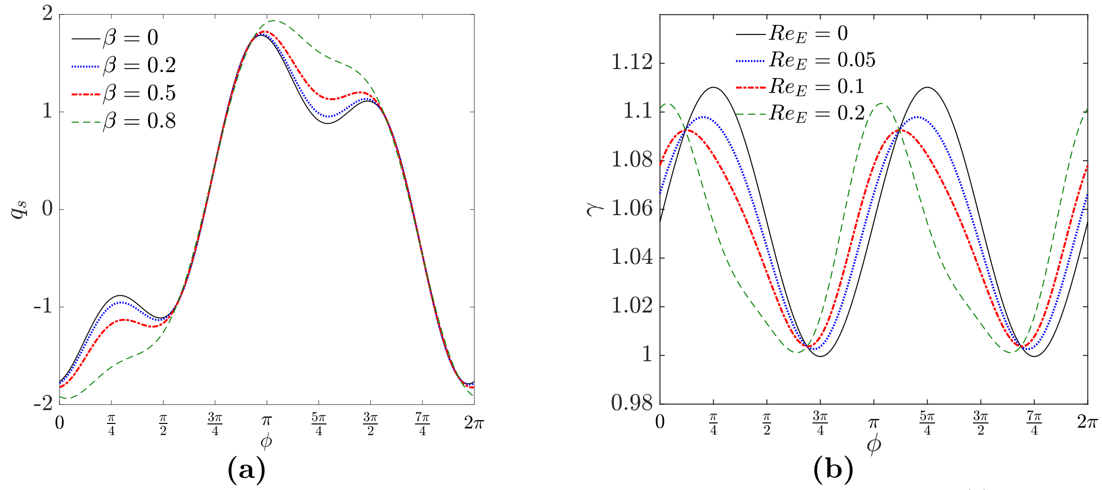

Figure S-3: (a) Azimuthal variation of the surface charge density ($q_S = q_S^{(0)} + Re_E\, q_S^{(Re_E)}$) for different values of the surface elasticity parameter, β. (b) variation of the surface tension ($\gamma = \gamma^{(0)} + Ca\,\gamma^{(Ca)} + Ca Re_E\,\gamma^{(Re_E)}$) for different values of electric Reynolds number (Re_E). The demonstrations are for system-C. Parameters are chosen as $Re_E = 0.2, M = 2, k = 1, \Phi_t = \pi/4$ and $Ca = 0.2$.

S-6. Variation of interfacial velocity and electrical traction

Here we exemplify the coupled consequence of charge convection and Marangoni stress on the flow field by showing the variation in the azimuthal components the drop velocity and electrical traction at the interface in figures S-4.

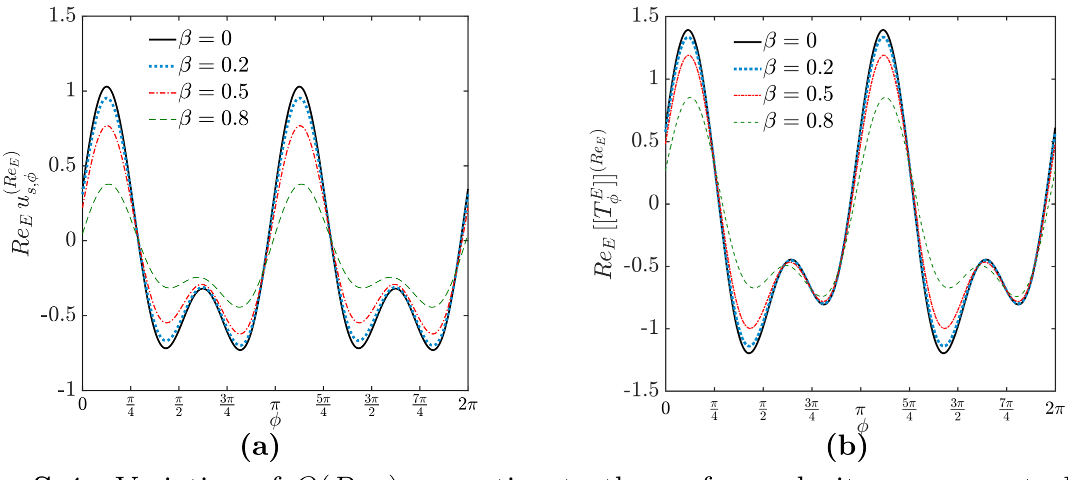

Figure S-4: Variation of $O(Re_E)$ correction to the surface velocity component, $Re_E\, u_{S,\phi}^{(Re_E)}$ and electrical traction component at the drop surface, $[[T_\phi]]^{(Re_E)} = T_\phi^{E(Re_E)}\big|_c - T_\phi^{E(Re_E)}\big|_d$ for different surface elasticity parameter, β. Here the demonstration os for system-C, while rest of the parameters are $M = 2, Re_E = 0.2, \Phi_t = \pi/4$ and $k = 1$.

S-7. Surfactant effect on electrohydrodynamic drop deformation

In order to quantify the deformation behaviour of the drop we define a deformation parameter in the plane of shear as follows, $\mathcal{D} = \dfrac{\max(r_s(\theta = \pi/2, \phi)) - \min(r_s(\theta = \pi/2, \phi))}{\max(r_s(\theta = \pi/2, \phi)) + \min(r_s(\theta = \pi/2, \phi))}$. Another important quantification of the drop deformation is the drop inclination angle which can be defined in the $x-y$ plane as the angle ϕ corresponding to the maximum value of r_s for $\theta = \pi/2$ and is given as $\varphi_d = \frac{1}{2}\tan^{-1}(\hat{L}_{2,2}/L_{2,2})$. In comparison to the case when only a simple shear flow is present (Li & Pozrikidis, 1997), the electrical effects (with $\Phi_t = \pi/4, M = 2$) increases the deformation parameter ($\mathcal{D}$) for system-B. In contrast, for system-C the initial prolate shape (with respect to the applied electric field direction along $\Phi_t = \pi/4$) of the drop under simple shear flow becomes a complete oblate one when electrical effects are present. This phenomenon is portrayed in the insets of the figures S-5(a) and (b)). In this section (figure S-5) we describe the drop shapes for different electrohydrodynamic systems. Also the variation of deformation parameter $\mathcal{D}$ with the surface elasticity number β is shown.

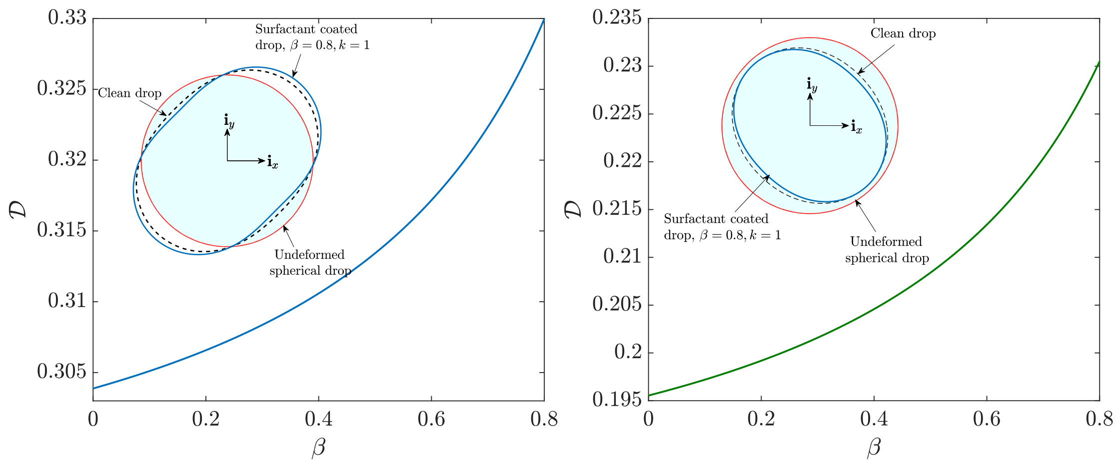

(a) System-B **(b)** System-C

Figure S-5: Effect of non-uniform surfactant distribution on the drop shape deformation in the plane of shear for systems B and C, respectively. The other parameters are $M = 2$, $Ca = 0.2$, $\Phi_t = \pi/4$.

References

Bandopadhyay, A., Mandal, S., Kishore, N. K. & Chakraborty, S. 2016 Uniform electric-field-induced lateral migration of a sedimenting drop. *J. Fluid Mech.* **792** (2016), 553–589.

Barths-Biesel, D. & Acrivos, A. 1973 Deformation and burst of a liquid droplet freely suspended in a linear shear field. *J. Fluid Mech.* **61**, 1.

Happel, J & Brenner, H 1981 *Low Reynolds number hydrodynamics*. Springer.

Hetsroni, G. & Haber, S. 1970 The flow in and around a droplet or bubble submerged in an unbound arbitrary velocity field. *Rheol. Acta* **9** (4), 488–496.

Lamb, H. 1975 *Hydrodynamics*, 6th edn. Cambridge University Press.

Li, X. & Pozrikidis, C. 1997 The effect of surfactants on drop deformation and on the rheology of dilute emulsions in Stokes flow. *J. Fluid Mech.* **341** (1997), 165–194.

MANDAL, S. & CHAKRABORTY, S. 2017 Uniform electric-field-induced non-newtonian rheology of a dilute suspension of deformable newtonian drops. *Phys. Rev. Fluids* **2**, 093602.

MANDAL, S., DAS, S. & CHAKRABORTY, S. 2017 Effect of marangoni stress on the bulk rheology of a dilute emulsion of surfactant-laden deformable droplets in linear flows. *Phys. Rev. Fluids* **2**, 113604.

SCHOWALTER, W. R., CHAFFEY, C. E. & BRENNER, H. 1968 Rheological behavior of a dilute emulsion. *Journal of colloid and interface science* **26** (2), 152–160.

TAYLOR, G. I. 1932 The viscosity of a fluid containing small drops of another fluid. *Proc. R. Soc. Lond. A* **138** (834), 41–48.

VLAHOVSKA, P. M. 2011 On the rheology of a dilute emulsion in a uniform electric field. *J. Fluid Mech.* **670**, 481–503.

VLAHOVSKA, P. M., BŁAWZDZIEWICZ, J. & LOEWENBERG, M. 2009 Small-deformation theory for a surfactant-covered drop in linear flows. *J. Fluid Mech.* **624**, 293–337.